Proceedings of the 11th International Conference on Manufacturing Research (ICMR2013), Cranfield University, UK, 19th – 20th September 2013, pp 239-244

CHARACTERISATION OF THE RELATIONSHIP BETWEEN SURFACE TEXTURE AND SURFACE INTEGRITY OF SUPERALLOY COMPONENTS MACHINED BY GRINDING

Quanren Zeng [a, b]
[a] School of Mechanical Engineering
Northwestern Polytechnical University
Xi'an, 710072, Shaanxi, China
[b] Department of Design, Manufacture and Engineering Management
University of Strathclyde
Glasgow, G1 1XJ, UK
quanren.zeng@strath.ac.uk

Yi Qin
Department of Design, Manufacture and Engineering Management
The University of Strathclyde
Glasgow, G1 1XJ, UK
qin.yi@strath.ac.uk

Geng Liu
School of Mechanical Engineering,
Northwestern Polytechnical University
Xi'an, 710072, Shaanxi, China
npuliug@nwpu.edu.cn

Lan Liu
School of Mechanical Engineering,
Northwestern Polytechnical University
Xi'an, 710072, Shaanxi, China
liulan@nwpu.edu.cn

ABSTRACT

The surface texture of a machined component is influenced largely by the processing parameters used during machining and hence, there is a relationship between both the formation of the surface texture and surface integrity of the machined component. In the study to be reported in this paper, GH4169, a hard-to-cut superalloy, widely used in aero-engines, was selected for a detailed investigation into the relationship between the surface texture and the component-performance (surface integrity) of the machined components for which a series of grinding experiments with different grinding-wheels and grinding parameter-values was carried out in order to quantitatively analyze variations of the surface roughness with processing parameters. Further, considering that the features of the ground-surfaces measured are of a random nature, statistic properties of the produced surfaces were revealed and characterised with power spectral density function (PSD) and auto-covariance function(ACV) method respectively.

Keywords: surface texture, grinding process parameters, power spectral density, auto-covariance function.

1 INTRODUCTION

Surface texture, also known as surface topography, is one of the typical surface integrity characteristics for performance evaluation and usually quantitatively denoted by surface roughness parameters such as average roughness R_a, root mean square roughness R_q, ten-point height R_z etc.. Surface integrity provides an effective means for characterizing and assessing the surface and subsurface features and their related functionalities. Different surface texture behaviour will directly cause variation of the surface integrity characteristics and consequent change of mechanical properties of the machined components.

The difficult-to-machine material GH4169, is a kind of nickel base superalloy and widely used in the aerospace and nuclear industry, with its unique combinations of properties such as high temperature strength, high hardness and high heat and corrosion-resistance. However, these exceptional aspects of performance oppositely pose a greater challenge to manufacturing engineers and make it more susceptible to the related manufacturing processes (Ezugwu, et al., 2003). Considering that the surface texture of a machined component is mainly affected by its machining

parameters, many researches have been carried out to find their relationship for different manufacturing processes and materials. For instance, Novovic *et al*. (2004) compared the surface topography and integrity effects on fatigue performance for conventional and non-conventional processed components. Ulutan and Ozel (2011) considered specifically the machining induced surface integrity for aero-used Ti and Ni alloys. Ding *et al*. (2010) studied the creep feed grinding process effect on the grindability and surface integrity of Ni-base alloy when using CBN superhard wheels. Bushlya *et al*.(2012) researched how the turning scenarios will influence the machinability of Inconel 718 components with coated and uncoated PCBN tools. Jawahir *et al*. (2011) analyzed and reviewed the works about surface texture effect on the surface integrity and related functional performance during material removal processes carried out in the last 3 years.

Although the 2D surface roughness parameter R_a, is the most-widely used index and technical requirement for quality of mechanical components, there are other statistical functions which describe specific surface performance more accurately and comprehensively than R_a does. The Auto-correlation function (ACF) is a statistic function describing the space interval over which a correlation or similarity is in the surface profile or texture (Griffiths 2001). It actually tells if the surface studied has repetitive features. The power spectral density function (PSD) decomposes the measured stochastic surface profile into different spatial frequencies and helps identify periodicities. By computing the amplitude of the frequency components that make up the surface, it provides more visual information than single-number parameters like R_a or R_q. Mathematically, the PSD is the square of the Fourier transform of the original surface profile and it can be discretely expressed as follows:

$$PSD(f) = \frac{d_0}{N}\left|\sum_{j=1}^{N} Z_j \cdot \exp[-i \cdot 2\pi f (j-1) d_0]\right|^2 \tag{1}$$

where $i=\sqrt{-1}$, d_0 the sampling length, Z_j the amplitude function of surface, f the spatial frequency. Auto-covariance (ACV) is the inverse Fourier transform of the PSD data. In an ACV analysis, the measuring system shifts the data laterally and compares it with the original data. The ACV plot indicates how well the shifted surface correlates with the original. This gives a measure of the randomness of the surface.

In this paper, the surface texture and integrity of ground GH4169 components have been studied by using different grinding wheels and processing parameters. Their effects on the surface roughness for the ground components are investigated by single factorial experiments. Furthermore, the random nature of the 3D surface texture is also analyzed with some statistical functions like PSD and ACV, which are able to provide more abundant and visual information for geometry characterization and performance evaluation.

2 MATERIAL AND EXPERIMENTAL PREPARATION

The material researched in this work is GH4169 Ni-base superalloy, the composition of which is presented in Table 1(Gu *et al*. 2001). Two types of grinding wheels are used within the study for the performance evaluation of GH4169. The first is a conventional single alundum wheel with Al_2O_3 abrasive grains and the second is a superhard CBN wheel with cubic boron nitride abrasive grains. The grit size of these two wheels is 80#. The diameter of the final cylindrical workpieces are 30mm and their length are 100mm. The abrasive debris morphology and ground surfaces of components are measured by using scanning electron microscopy and 3D optical interferometer.

Table 1: The composition of GH4169 superalloy (%)

C	Cr	Ni	Co	Mo	Al	Ti	Nb	Fe
≤ 0.08	17-21	50-55	≤ 1	2.8-3.3	0.2-0.6	0.65-1.25	4.75-5.5	other
Mn	B	Mg	Si	P	S	Cu	Ca	Pb
<0.35	<0.006	<0.01	<0.35	<0.015	<0.015	<0.30	<0.01	0.0005

3 PROCEDURE

Grinding experiments were arranged to investigate the direct influences of wheel property and machining parameters on surface texture and integrity for GH4169 components.

In order to take account of the distinct abrasive grain effects of the grinding wheel on the machined surface texture, a conventional Al_2O_3 grinding wheel and a superhard CBN grinding wheel are employed to grind the components with the same grinding parameters Before the grinding tests, the wheels are trued by using a single-point diamond dresser to keep them with the same extent of sharpness. The abrasive debris morphology collected from the two grinding processes are studied and compared with each other by using SEM analysis.

To consider the operational grinding parameters' effect on the surface roughness, two kinds of experiments are designed. Firstly, two components are externally ground with Al_2O_3 wheel at higher and lower material removal rate to determine their respective actions on the machined surface texture. The grinding parameters producing higher material removal rate are v_s=30m/s, a_p=0.025mm, v_w=10m/min, f_a=1mm/r; while the corresponding grinding parameter for lower material removal rate are v_s=20m/s, a_p =0.005mm, v_w=10m/min, f_a=1mm/r. The surface texture of machined components are observed and contrasted by using SEM micrographs. Secondly, a series of single-factorial experiments was designed to separately investigate the variation of surface roughness R_a with the 4 main grinding parameters during the external traverse-grinding with the same grinding wheel and lubrication condition. When one grinding parameter is under study, the others are held constant.

4 RESULTS AND ANALYSIS

4.1 Grinding wheel property's effect

The Al_2O_3 wheel and CBN wheel were used to grind cylindrical components with the same processing condition. As shown in Fig.1(a)-(d), when the Al_2O_3 wheel is used, the debris collected are mostly thin and long strips. They are comparatively uniform and even-proportioned in size. However, when the CBN grinding wheel is used to process the GH4169 component, the size of the abrasive dusts become greater and the debris is extremely irregular the shape, having a semi-lunar appearance. Furthermore, it seems that the debris has been over-pressured, then squeezed, and then torn off from the component's surface, rather than having been normally cut off by the edges of the grains.

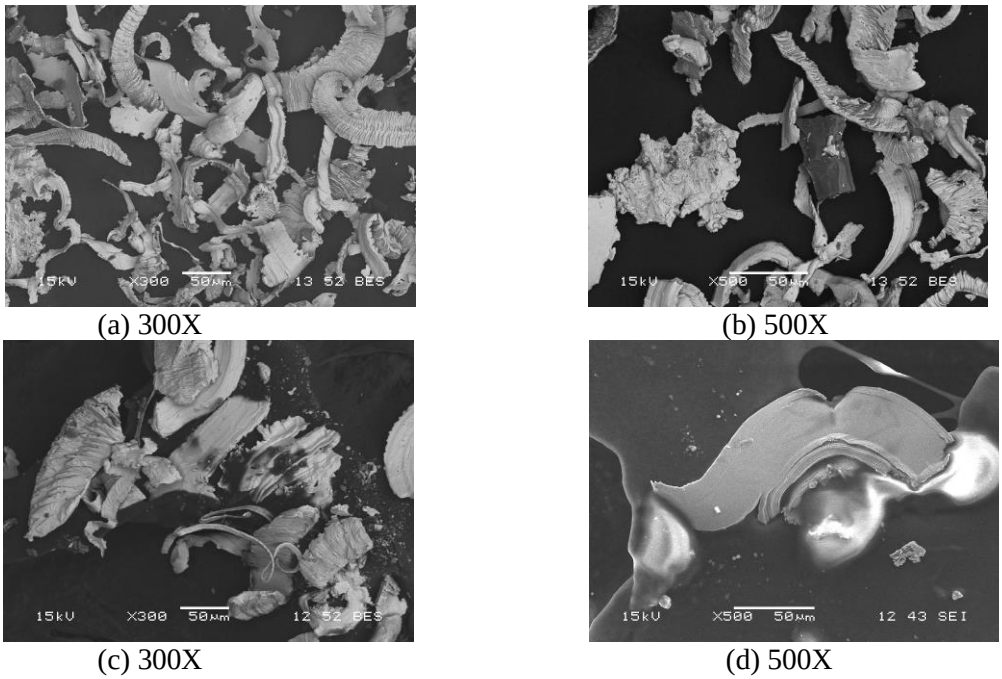

(a) 300X (b) 500X

(c) 300X (d) 500X

Figure 1: Debris morphology: (a)-(b) removed by Al_2O_3 wheel; (c)-(d) removed by CBN wheel

4.2 Processing parameters' effect

The effect of grinding with different material removal rates with the Al_2O_3 wheel is also investigated. Fig.2 compares the surface texture produced by grinding at higher material removal rate(when v_s=30m/s, a_p=0.025mm, v_w=10m/min, f_a=1mm/r) and lower material removal rate(when v_s=20m/s,

a_p=0.005mm, v_w=10m/min, f_a=1mm/r). If the material removal rate is lower, the ground surface is composed of parallel and clear scratches, where the lateral spacing between scratches is around 10μm. The walls of scratches are clearly visible and remain integrated even when magnified 2000X. However, if the material removal rate is higher, increased discontinuities, irregularities, defects or deposits, scratches and burrs can be found on the ground surface. There are only a few regular feed marks and at some local areas the machined surface experiences severe plastic deformation and the grinding scratches or lays are smeared and hard to discern: the appearance suggests that some component's material has firstly been ripped off then recombined on the machined surfaces. Many abrasive grains from the Al_2O_3 wheel (see the black particles in Fig.2(g)) are also broken off and attached to the local surface of laps or folds.

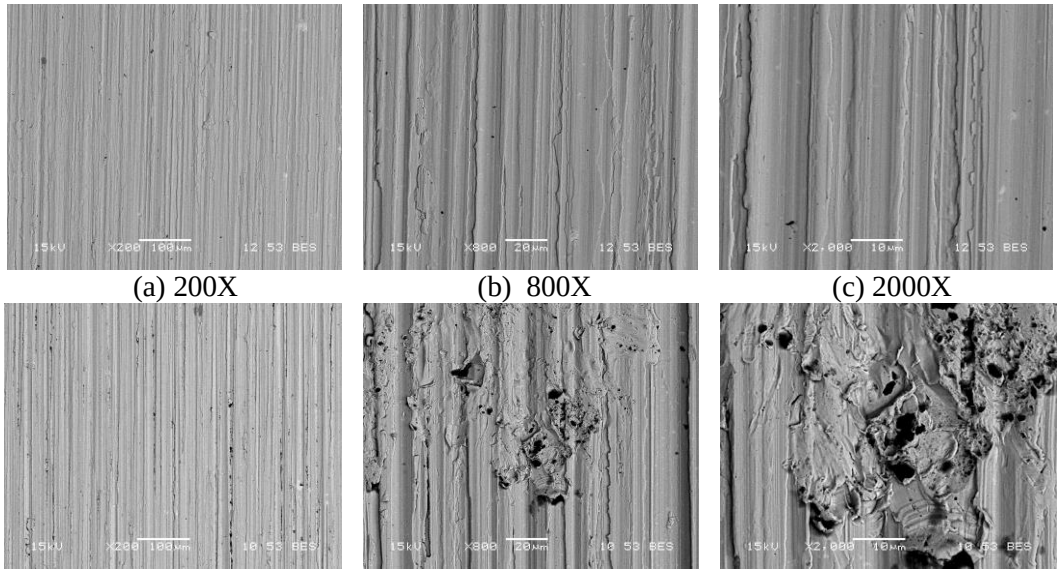

(a) 200X (b) 800X (c) 2000X

(e) 200X (f) 800X (g) 2000X

Figure 2: Surfaces ground by (a)-(c) lower and (e)-(f) higher material removal rates

Single-factorial experiments were also carried out to investigate how the surface roughness varies with each main grinding parameter of external grinding. Fig.3(a) depicts that with the increase of workpiece speed v_w from 8m/min to 43.3m/min while other parameters are held constant (v_s=25m/s, a_p=0.015mm, f_a=1.0mm/r), the surface roughness R_a fluctuates slight but takes on a generally declined trend. Fig.3(b) shows that if the feed f_a rises from 0.5mm/r to 3mm/r, the R_a value will increase within the given grinding parameter range. Fig.3(c) demonstrates that the surface roughness R_a drops slowly with the increase of wheel speed v_s from 15m/s to 30m/s. However, it then soars to 0.33μm when the wheel speed v_s reaches to 35m/s, nearly twice the value for lower wheel speed v_s=30m/s.

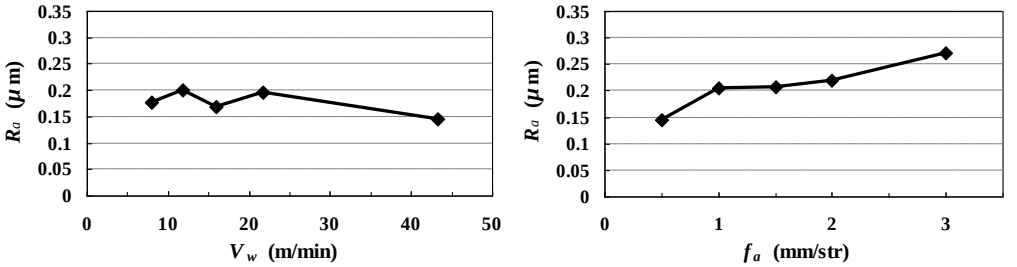

(a) v_s=25m/s, a_p=0.015mm, f_a=1.0mm/r (b) v_s=25m/s, a_p=0.015mm, v_w=16m/min

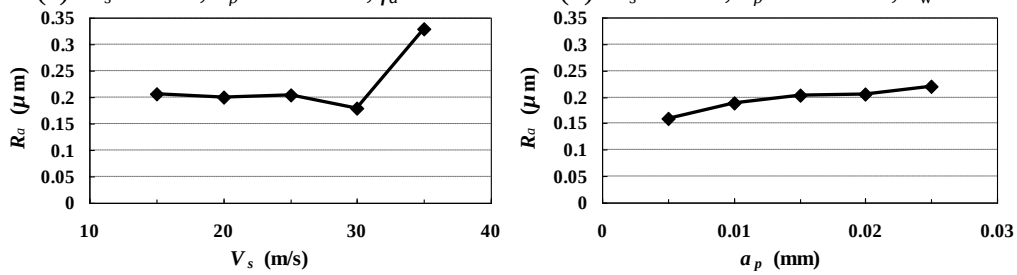

(c) v_w=16m/min, a_p=0.015mm, f_a=1.0mm/r (d) v_s=25m/s, v_w =16m/min, f_a=1.0mm/r

Figure 3: Grinding parameters effect on the surface roughness

The main reason for this abrupt inflexion may be the rapid increase of grinding temperature and force when the wheel speed exceeds a certain value like v_s=35m/s. Fig.3(d) indicates that with the increase of a_p from 0.005mm to 0.025mm, the surface roughness R_a will increase gradually and monotonously. These results shows that the depth of cut a_p and feed f_a usually maintain a consistent effect on the variation of surface roughness values.

4.3 PSD and ACV analyses of Ground surface

Fig.5 illustrates the measured 3D surface and related 2D profile of component ground with Al_2O_3 wheel at v_s=25m/s, v_w=16m/min, a_p=0.015mm and f_a=1.0mm/r by using a 3D optical interferometer. The sampling length is 165.63μm and the scanned array are 736×480. There are traces and lays parallel to the grinding direction X on the 3D ground surface which means the surface takes on periodic and anisotropic features along Y axis to some extent within the measurement range. Fig.5(a)-(b) shows the PSD curve fluctuates to zero as the spatial frequency increase along Y direction, and there are several spikes indicating the ground surface having some finer waveform lengths along with the base wavelength of $\lambda_f=1/f_z\approx0.05$mm. ACV is the inverse Fourier transform of the PSD data. In Fig.5(c)-(d), the ACV in the Y direction rapidly declines to and fluctuates around zero, which means the ground surface is less auto-correlated and is of random nature along Y direction.

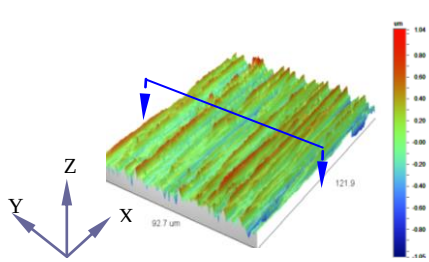

(a) 3D surface texture(R_a=0.208μm)

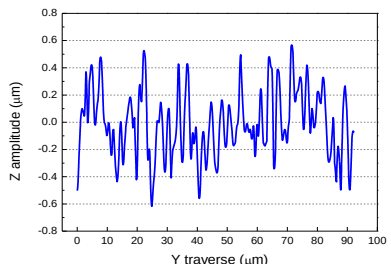

(b) 2D profile

Figure 4: Ground surface topography

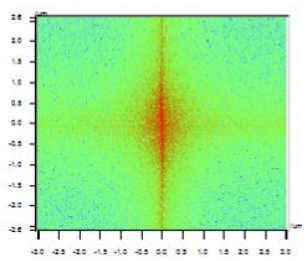

(a) PSD plot

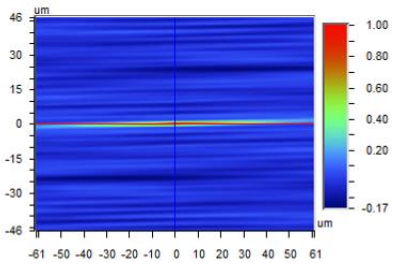

(c) ACV Plot

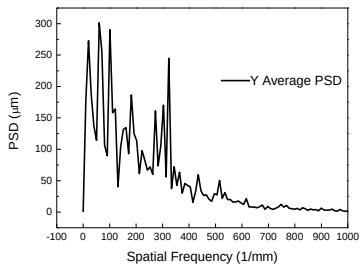

(b) Average PSD along Y

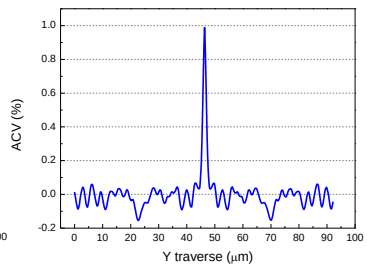

(d) Average ACV along Y

Figure 5: PSD and ACV of the measured surface

5 DISCUSSION

The selection of an appropriate abrasive wheel and grinding parameters for a specific workpiece material is vital to the final surface quality of machined components. For the machining-sensitive GH4169 material, it can be seen from Fig.1 that the chips and debris removed by the Al_2O_3 wheel are comparatively thinner and more regular than those removed by the CBN wheel under the same grinding parameters and conditions researched. Actually, the size and shape of the debris indirectly reflect the corresponding precision and behavior of machined surface. It may naturally be imagined that the GH4169 components ground by the Al_2O_3 abrasive wheel usually produce better surface quality and lower roughness than those ground by the CBN abrasive wheel within the grinding parameter range studied. From the point of view of energy input level, it means the plastic deformation during the grinding process with the CBN wheel is more complex and intensive than that with Al_2O_3 wheel, which indicates that the CBN wheel will cause more in-depth and remarkable

action on the final machined surface than what Al_2O_3 grinding wheel produces under the identical processing parameters studied.

A large grinding parameter will increase the material removal rate and improve the productivity. For a hard-to-machine material like GH4169, high material removal rate parameters may be readily employed to speed the machining process and reduce the machining cost. However, a high material removal rate may be prone to cause local areas of the ground surface to suffer severe plastic deformation and endure consequent much higher grinding force and temperature. As Fig.2 shows, the measured mean surfaces roughness ground with lower and higher material rate are R_a=0.21μm and R_a=0.41μm. The surface ground with higher material rate has more profound subsurface transformation in addition to obvious surface defect and deformation. This will constitute a potential surface integrity danger for the machined component in service. According to the SEM/EDS analysis, it was found the composition of the black particles in Fig.2(f) are Al and O, so it can be inferred that they are Al_2O_3 grains broken off from the grinding wheel. This may be mainly caused by the rapid increase of grinding force and heat between the interface of the grinding wheel and workpiece when using high material removal rate. This will deteriorate the surface status, lead to high R_a value and makes more abrasive grains break off from the wheel and become attached to the machined surface. To control the surface roughness and integrity of the ground components, the main operational grinding variables are also the key. For the external traverse grinding within the grinding parameters range researched, the results shows that the depth of cut a_p and feed f_a usually have a consistent effect on the variation of surface roughness values.

6 CONCLUSION

This paper presents results in term of surface texture and integrity when grinding GH4169 difficult-to-machine superalloy. Grinding experiments with different grinding wheels and corresponding grinding parameters have been carried out to quantitatively study the effect and variation of surface roughness with specific manufacturing processes. 3D surface texture and its statistical properties like PSD and ACV were observed and analyzed with the white light interferometer technique which further enriches the functional description and characterization of the machined surface. The results give engineers a general guide to the adjustment of grinding conditions and control surface roughness and integrity for the final functional performance when machining superalloy GH4169.

ACKNOWLEDGMENTS

The research is supported by the National Natural Science Foundation of China (51275423) and 111 Project (B13044). The authors would also like to thank Professor Jingxin Ren and Mr Xinchun Huang for their helpful discussion relating to the experiment, and Professor Frank Travis for his assistance in proof reading of this article.

REFERENCE

Bushlya, V., J. Zhou, and J. E. Stahl. 2012. Effect of Cutting Conditions on Machinability of Superalloy Inconel 718 During High Speed Turning with Coated and Uncoated PCBN Tools. *Procedia CIRP* 3: 370-375.

Ding, W., J. Xu, Z. Chen, H. Su, and Y. Fu. 2010. Grindability and Surface Integrity of Cast Nickel-based Superalloy in Creep Feed Grinding with Brazed CBN Abrasive Wheels. *Chinese Journal of Aeronautics* 23(4):501-510.

Ezugwu, E. O., J. Bonney, and Y. Yamane. 2003. An overview of the machinability of aeroengine alloys. *Journal of Materials Processing Technology* 134(2): 233-253.

Gu, M., et al. 2001. *China Aeronautical Materials Handbook*. 2rd ed. Beijing: China Standard Press.

Griffiths, B. 2001. *Manufacturing Surface Technology–Surface integrity and functional performance*. London: Penton Press

Jawahir, I. S., E. Brinksmeier, R. M'Saoubi, D. K. Aspinwall, J. C. Outeiro, D. Meyer, D. Umbrello, and A. D. Jayal.. 2011. Surface integrity in material removal processes: Recent advances. *CIRP Annals - Manufacturing Technology* 60(2): 603-626.

Novovic, D., R.C. Dewes, D.K. Aspinwall, W. Voice, and P. Bowen. 2004. The effect of machined topography and integrity on fatigue life. *International Journal of Machine Tools and Manufacture* 44: 125-134.

Ulutan, D., and T. Ozel. 2011. Machining induced surface integrity in titanium and nickel alloys: A review. *International Journal of Machine Tools and Manufacture* 51(3): 250-280.